Relaxation of intense inhomogeneous charged beams

R. P. Nunes, R. Pakter, F. B. Rizzato, A. Endler, and E. G. Souza

Citation: Physics of Plasmas **16**, 033107 (2009); doi: 10.1063/1.3091914
View online: http://dx.doi.org/10.1063/1.3091914
View Table of Contents: http://scitation.aip.org/content/aip/journal/pop/16/3?ver=pdfcov
Published by the AIP Publishing

Relaxation of intense inhomogeneous charged beams

R. P. Nunes,[a] R. Pakter,[b] F. B. Rizzato,[c] A. Endler,[d] and E. G. Souza[e]
Instituto de Física, Universidade Federal do Rio Grande do Sul, Caixa Postal 15051, 91501-970 Porto Alegre, Rio Grande do Sul, Brazil

(Received 13 October 2008; accepted 9 February 2009; published online 17 March 2009)

This work analyzes the dynamics of inhomogeneous, magnetically focused high intensity beams of charged particles. Initial inhomogeneities lead to density waves propagating transversely in the beam core, and the presence of transverse waves eventually results in particle scattering. Particle scattering off waves in the beam core ultimately generates a halo of particles with concomitant emittance growth. Emittance growth indicates a beam relaxing to its final stationary state, and the purpose of the present paper is to describe halo and emittance in terms of test particles moving under the action of the inhomogeneous beam. To this end an average Lagrangian approach for the beam is developed. This approach, aided by the use of conserved quantities, produces results in nice agreement with those obtained with full *N*-particle numerical simulations. © *2009 American Institute of Physics*. [DOI: 10.1063/1.3091914]

I. INTRODUCTION

Magnetically focused beams of charged particles can relax from nonstationary to stationary flows with associated emittance growth and concomitant halo formation.[1] Gluckstern[2] showed that initial envelope oscillations of mismatched homogeneous beams induce formation of large scale resonant islands beyond the beam border:[3,4] Beam particles are captured by the resonant islands resulting in emittance growth and relaxation. A closely related question concerns the mechanism of beam relaxation and the associated emittance growth when the beam is not homogeneous, as frequently happens in beam transport channels.[1,5] On general grounds of energy conservation one again concludes that beam relaxation takes place when the coherent fluctuations of beam inhomogeneities are converted into microscopic kinetic energy, as shall be detailed along the paper.

Recent investigation of inhomogeneous beams shows that relaxation comes about as a consequence of particle scattering off density waves in the beam.[6] Scattering particles initially move in phase with the macroscopic density fluctuations, drawing their energy from the propagating wave fronts and converting it into microscopic kinetic energy. For ultracold, or crystalline beams, the process amounts to the mechanism of pure wave breaking, where particles are first coherently accelerated to the velocity of the waves and then abruptly ejected from high density peaks. At the moment of ejection, spatial dependence of oscillatory frequency, a needed feature for wave breaking, has already turned the core into a highly incoherent state.[7,8]

In the present paper we focus attention on the case of space charge dominated but warmer beams. Under these conditions, resonant particles are already present at initial times due to thermal spread, and the entire relaxation process is smoother. In contrast to the crystalline case, here particles gain energy while the core still displays coherence. In any case, ejected particles form a low density halo around the beam core, which ultimately increases beam emittance and relaxes the dynamics. Due to its low density the ejected population can be very accurately described as a set of test particles. It is thus of importance to describe the motion of test particles as they are driven into the halo by core fluctuations. The core itself generically behaves as an oscillatory drive, the details of which depend on the particular instance investigated. While in homogeneous cases the core is occasionally modeled as a breathing flattop charge distribution, corresponding models for oscillating inhomogeneous beams are less frequent.

The first aim of this paper is therefore to construct a model for the inhomogeneous oscillating core. To do that we make use of a Lagrangian approach with which one can describe its dominant nonlinear oscillatory mode. Then, as the core is coupled to test particles, one can give a good account of the latter's distribution in phase space. One further adds the help of conserved quantities to obtain saturated quantities such as the relaxed emittance, and in the final step we show that the modeled emittance agrees well with the one obtained from particle simulations.

The paper is organized as follows. In Sec. II we discuss general features of the problem and introduce the model for the oscillating core and for test particles. In Sec. III we make use of the model aided by use of conserved quantities to estimate the structure of the final relaxed state; comparisons are then made with full particle simulations. In Sec. IV we draw our conclusions.

II. THE MODEL AND INITIAL ANALYSIS

We consider solenoidal focusing of space charge dominated beams propagating along the transport axis, defined as the z axis of our reference frame. The beam is initially cold with very small emittance, and is azimuthally symmetric around the z axis. Our problem is then to describe the average oscillatory motion of the beam core and how it drives test particles to form halo with subsequent beam relaxation.

[a]Electronic mail: rogerpn@if.ufrgs.br.
[b]Electronic mail: pakter@if.ufrgs.br.
[c]Electronic mail: rizzato@if.ufrgs.br.
[d]Electronic mail: aendler@if.ufrgs.br.
[e]Electronic mail: evertongs@if.ufrgs.br.

Considering full azimuthal symmetry, one can use Gauss' law in order to write the governing equation for any particle in the beam,[7,9–11]

$$r'' = -\kappa r + \frac{Q(r)}{r}, \tag{1}$$

primes indicating derivative with respect to the longitudinal z coordinate which for convenience we shall also refer to as "time." The focusing factor is $\kappa \equiv (qB/2\gamma m\beta c^2)^2$, where B is the axial, constant, focusing magnetic field. $Q(r) = KN(r)/N_t$ is the particle-averaged measure of the charge contained between the origin at $r=0$ and the position $r(z) = r$, N_t is the total number of beam particles per unit axial length, $N(r)$ is the number of particles up to r, and $K = N_t q^2/\gamma^3 m\beta^2 c^2$ is the beam perveance. q and m denote the beam particle charge and mass respectively, and $\gamma = (1-\beta^2)^{-1/2}$ is the relativistic factor with $\beta = v_z/c$. v_z is the constant axial beam velocity and c is the speed of light.

A. Density oscillations of the core

We recall that we are interested in slightly thermal beams where particles begin to move away from the core while it still oscillates coherently. Particles left in the core are thus approximately described in terms of a charged fluid where trajectories of individual fluid elements do not intercept each other during the dynamics. In other words, for a particular position at a particular time, one can ascribe a unique velocity for all particles sitting there. Particles whose trajectories do cross each other are halo particles and form the kinetic part of the full particle distribution. This kinetic portion of the distribution will be handled later.

Since the core is assumed to be a fluid with negligible random motion, the amount of charge that a core particle sees at any time equals the charge initially seen at $z=0$. In other words, if a core particle evolves from r_0 at $z=0$ to a new position r at time z, we consider $Q(r,z) = Q(r_0)$. r_0 is in fact the Lagrangian coordinate of the core particle,[12] which means that the solution to Eq. (1) can be written parametrically in terms of r_0 in the convenient form $r = r(r_0, z)$. Once again we emphasize that the amount of charge $Q(r)$ seen by the fluid element inside the region $0 < r \leq r(z)$ remains unaltered at $Q(r_0)$, independently of time z. This is of fundamental importance since from Gauss' law this is the charge that exerts the force on the fluid element.

Expression (1), adapted for core particles according to the preceding comments, can be readily obtained from the single-particle Lagrangian $\mathcal{L}$

$$\mathcal{L}(r,r') = \frac{r'^2}{2} - \kappa\frac{r^2}{2} + Q(r_0)\ln(r), \tag{2}$$

with help of Euler–Lagrange equations. In our system one has a multitude of N_t particles, as mentioned, and the full transverse Lagrangian takes the form

$$L = \int \mathcal{L}(r,r')n(r_0)d^2r_0, \tag{3}$$

where what one is doing is to multiply the single-particle Lagrangian at coordinate r by the number of particles evolving from $r(z=0) = r_0$ to $r(z) = r$, $n(r_0)d^2r_0$, and integrating over all possible initial conditions. Recalling that since we are dealing with core particles, the amount of charge seen by a particle at any time z equals that at $z=0$. This explains the presence of the term $Q(r_0)$—computed at r_0—in Eq. (2).

At the present point we would like to invoke average Lagrangian techniques.[13] The purpose here would be to produce an average formalism that could provide an easy way into obtaining the nonlinear frequency and the amplitude of the dominant oscillatory mode of the core. With this approximate core dynamics serving as a drive for test particles, we shall finally attempt to investigate halo formation and the corresponding basic features of the relaxed state.

The general idea of the average Lagrangian is to suppose a trial shape for the density $n = n[r, \chi(z)]$, where z dependence comes through an amplitude factor $\chi = \chi(z)$ to be determined. Then one proceeds to integrate Eq. (3) over r_0 and apply the Euler–Lagrange method of stationary action to obtain a governing equation for the density fluctuation amplitude $\chi(z)$. This will complete the description for the core dynamics.

Let us list in some detail the most critical steps needed to achieve our goal.

(i) We first of all note that given continuity, fluid elements must evolve obeying the constraint $n(r_0)d^2r_0 = n[r,\chi(z)]d^2r$. Once the trial function $n[r,\chi(z)]$ has been defined, this step enables to write $n(r_0)d^2r_0$ in Eq. (3) explicitly in terms of the radial coordinate r and the respective differential.

(ii) In addition to that, continuity can be used once again, now in terms of the azimuthally symmetric continuity equation

$$\frac{\partial n}{\partial z} + \frac{1}{r}\frac{\partial}{\partial r}(rnv) = 0, \tag{4}$$

to extract an expression for the velocity r' in terms of the coordinate and time:

$$r' = -\frac{1}{rn}\int_0^r r\frac{\partial}{\partial z}n[r,\chi(z)]dr \equiv v = v[r,\chi(z)]. \tag{5}$$

(iii) We finally note that since $Q(r_0) = Q[r,\chi(z)] = (K/N_t)N[r,\chi(z)]$ from Eq. (1) and associated definitions, the charge Q in $\mathcal{L}$ can be also explicitly written in terms of the radial coordinate r once we integrate the density n to find $N[r,\chi(z)]$.

The steps above guarantee that, given the density $n[r,\chi(z)]$, we can change the integration variable in Eq. (3) from r_0 to r and perform the integration so what we need now is the *ansatz* for the density. As initial condition we impose a parabolic type perturbation of the form $n(r \leq r_c) = \rho_h[1 + \chi(2r^2/r_c^2 - 1)]$ [with $n(r > r_c) = 0$], where ρ_h is the average beam density and r_c is the beam core radius. Then we assume that as the density wave evolves in the core it can be represented in the form

$$n[r,\chi(z)] = \rho_h\left[1+\chi(z)\left(2\frac{r^2}{r_c^2}-1\right)\right], \tag{6}$$

where now we let the amplitude to become a function of time z. The ansatz represents a compressive-rarefactive wave and gives an accurate account of the density fluctuations for short times following the initial state. Only for much longer periods, effects associated with spatial dependence of oscillatory frequency become more noticeable.[6,7] As explained earlier, we intend to apply the theory in case of space charge dominated, but not ultracold fully crystalline beams. In this case some stray particles detached early from the beam core gain energy while the core still oscillates in a coherent fashion. Since these first evaporated particles are the ones that absorb maximum energy and define the halo boundaries in phase space, usage of expression (6) is justified.

The case of crystalline beams was investigated in a previous paper.[6] Under these conditions particles detach from the core only when wave breaking due to spatial dependence of the oscillatory frequency takes place. Then, while the monochromatic ansatz (6) is in principle arguable, we shall comment later how the estimates can still be used.

We also choose $r_c=K/\kappa$ so particles at beam border are at equilibrium. Under this condition the beam displays internal oscillations but keeps its radius unaltered during initial stages. This reduces the action of Gluckstern's resonances and therefore enhances the effects of density oscillations which is our focus here.

With help of the ansatz and all steps detailed above, we can fully integrate Eq. (3) with respect to r and make use of Euler–Lagrange equations applied to the remaining function $\chi=\chi(z)$,

$$\frac{d}{dz}\left(\frac{\partial L}{\partial \chi'}\right)-\frac{\partial L}{\partial \chi}=0, \tag{7}$$

to obtain a closed expression for the amplitude

$$\chi''(z)=F[\chi(z),\chi'(z)], \tag{8}$$

where the specific form of the involved function F, obtainable from the Euler–Lagrange procedures, is written below:

$$F=\left[r_c^2\left(3[\chi(z)+1][\chi(z)^2+\chi(z)-4]\left\{\log\left(\frac{1}{1-\chi(z)}\right)+\log[\chi(z)+1]\right\}-2\chi(z)\{\chi(z)[2\chi(z)-9]-12\}\right)\chi'(z)^2\right.$$
$$\left.-16\chi(z)^5[2r_c^2+\chi(z)-2]\right]\Bigg/\left[2r_c^2\chi(z)\left(3[\chi(z)-1]\left\{\log\left[\frac{1}{1-\chi(z)}\right]+\log[\chi(z)+1]\right\}[\chi(z)+1]^2\right.\right.$$
$$\left.\left.+2\chi(z)\{[3-2\chi(z)]\chi(z)+3\}\right)\right]. \tag{9}$$

The dynamics of the modeled $\chi(z)$ should be tested against full simulations and it will be. However let us defer the testing until we have discussed in more depth tools used in these full simulations. For now let us look into our next issue on how to describe the dynamics of test particles.

B. Test particle orbits

As for test particles, Eq. (1) is applied with the restriction that $Q(r)$ contains only the core charge. This is equivalent to our assumptions on the diluteness of the halo, whereby the core drives test particles but is not acted upon by the latter.

As they interact with the beam, test particles feel the space charge action of the core up to their current position $r=r(z)$. In particular, test particles outside the beam see constant charge. Therefore the governing equation for those test particles can be written as

$$r''=-\kappa r+\begin{cases}K\dfrac{r[r_c^2+(r^2-r_c^2)\chi(z)]}{r_c^4}, & \text{if } r\le r_c,\\ K/r, & \text{if } r>r_c.\end{cases} \tag{10}$$

Equations (8) and (10) shall be solved simultaneously to obtain the dynamics of test particles.

III. ESTIMATES VERSUS FULL SIMULATIONS

A. Estimates based on conserved quantities and test particle dynamics

The χ dynamics, coming from a time independent one-dimensional Lagrangian, is completely integrable and periodic. Test particle motion can be thus represented in terms of a convenient Poincaré plot, where we record the pair of values $r(z)$ and $r'(z)$ each time $\chi(z)$ cycles one period.

One can also rescale radii, perveance and focusing factor so as to work with $K=\kappa=r_c=1$.[14] If in addition one selects $\chi(z=0)\equiv\chi_0=0.4$ and $\chi'(0)\to 0$ as typical initial conditions at beam entrance, one obtains the dynamics for the test particles as the scattered plot shown in Fig. 1.

Except for a resonance bubble near the origin, test particles distribute evenly over a limited region of phase space. One should expect, however, that the real phase space be a slightly shrunk version of the one in Fig. 1. This is so because in the real case core oscillations are damped, which reduces energy transfer into the halo. We obtain perhaps a better picture of the halo geometry by first computing the maximum velocity of test particles at $r=0$, and then forward integrating the orbit under the assumption that the beam has relaxed, i.e., by taking $\chi\to 0$. The result is the thick line

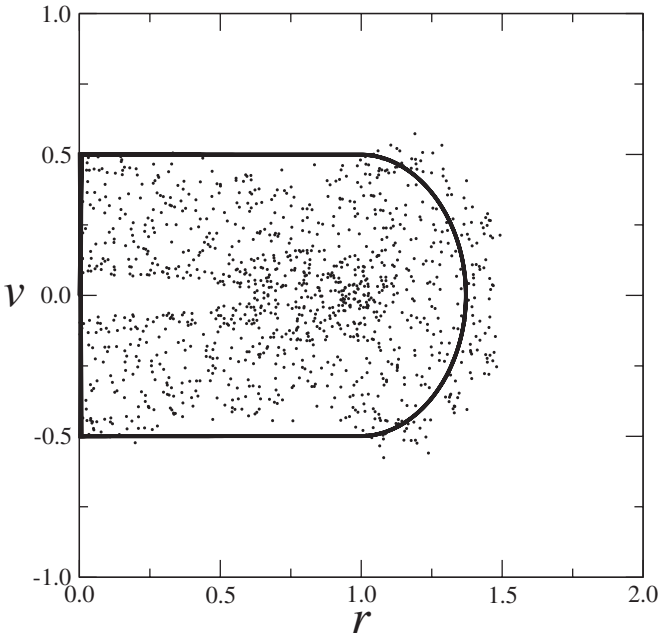

FIG. 1. Test particle dynamics (scattered dots) and bounding energy curve (thick line) for $\chi_0=0.4$.

present in Fig. 1. One key assumption of the model is that the halo will be homogeneously distributed over the region bounded by this maximum energy curve. In the case $\chi_0=0.4$ we find that the maximum radius and maximum velocity at $r=0$ reads $r_h\approx 1.36$ and $v_h\approx 0.504$, respectively.

What remains unknown up to the present point is the halo normalization—or the total number of halo particles—within the bounded domain. Only full knowledge of the distribution, layout and normalization, enables to calculate several quantities for the relaxed beam, including the emittance, an instrument of choice for beam diagnostics. We shall return to this specific issue of emittance later on.

Our approach to evaluate the halo density of the relaxed beam has been used before and shall be applied again here. Details can be found in a previous paper[14] and we shall outline the procedure here. Let us first of all introduce the conserved energy E,[10]

$$E=\frac{\langle r'^2\rangle}{2}+\kappa\frac{\langle r^2\rangle}{2}+\mathcal{E}(s)=\text{const}, \tag{11}$$

with angle brackets denoting average over particles. The first term of the middle expression represents kinetic energy, the second represents potential energy in the external magnetic field and $\mathcal{E}$ is the self-field energy. Self-field energy can be expressed in terms of the gradients of self-field potentials $\mathcal{E}=(1/4\pi K)\int d^2r|\nabla\phi|^2$, and the gradients can be obtained from Gauss' law as we integrate the radial Poisson equation

$$\nabla^2\phi=-\frac{2\pi K}{N_t}n(r). \tag{12}$$

The self-field term can be evaluated for an initial condition with a given density, and can be expressed as a function of the unknown halo fraction $f\equiv N_{\text{halo}}/N_t$ when we examine the relaxed state and consider a phase space of homogeneous density for the halo population. Average quantities appearing in the brackets of Eq. (11) can also be evaluated for initial and final states, with the proviso that in the final state they should be segregated into a core and halo contributions. To be more specific, an overall average $\langle g\rangle$ is to be written in the form $\langle g\rangle=(1-f)\langle g\rangle_{\text{core}}+f\langle g\rangle_{\text{halo}}$, where the subscripted averages are performed over the corresponding populations; $\langle g\rangle_{\{\text{core,halo}\}}=1/N_{\{\text{core,halo}\}}\Sigma_{i_{\{\text{core,halo}\}}}g_i$. The squared rms radius $\langle r^2\rangle$ is dealt with along these lines, and the velocity term $\langle r'^2\rangle$ is first expressed in terms of the relaxed emittance[10]

$$\varepsilon(z\to\infty)=2r_b\sqrt{\langle r'^2\rangle}, \tag{13}$$

which is then written in terms of the total beam radius r_b via the envelope equation $r_b''=-r_b+1/r_b+\varepsilon^2/r_b^2$, with $r_b''\to 0$ for the relaxed state and $r_b^2\equiv 2\langle r^2\rangle$.

If in addition we use sensible models for the core and halo, final emittance can be obtained as we enforce energy conservation by equaling relation (11) for both initial and final states. In our space charge dominated beams we assume that the core is a cold flattop entity extending up to a maximum radius r_c, and that the dilute halo displays constant density in phase space within the boundaries obtained by test particle calculations, as already mentioned. We will see shortly how the estimates compare with the full simulations.

B. Full simulations

Full particle simulations are then performed, where each particle is governed by Eq. (1) and where now the charge factor $Q(r)$ is *fully* and *self-consistently* evaluated with basis on all particles coordinates. Detailed information about the self-consistent method employed in the beam simulation shown here can be found in Ref. 14. In all cases we use $N_t=10\,000$ macroparticles, with the same parameters as used in the previous context of test particle dynamics; $K=\kappa=1$. As initial condition we use a density distributed according to expression (6) with a random velocity evenly laid upon the range $-0.1|v_{\text{directed}}|<r'<0.1|v_{\text{directed}}|$. Under our assumptions of space charge dominated systems, the velocity range is set as much narrower than the directed velocity v_{directed} acquired by the fluid. The directed velocity can be obtained as one inserts expression (6) into Eq. (5) and reads $v_{\text{directed}}\sim 0.1$ for $\chi_0=0.4$.

Our very first investigation with full simulations is on the usefulness of the core model. From Eq. (6) one can write χ in terms of the rms averages

$$\chi=6\left[\frac{\int r^2n(r,z)d^2r}{\int n(r,z)d^2r}-\frac{1}{2}\right]=6\left[\langle r^2\rangle-\frac{1}{2}\right]. \tag{14}$$

We then compare χ obtained from the model, let us call it χ_{model}, with the one obtained from Eq. (14) but with all averages based on full simulations, we call it $\chi_{\text{simulation}}$. The results, shown in Fig. 2 for $\chi_0=0.4$ up to a point where the first particles detach from the core, indicate that our modeling is accurate. One notices a small frequency mismatch as time progresses, but both the frequency and amplitude differences between model and simulations remain small until much later times where a large portion of particles is already

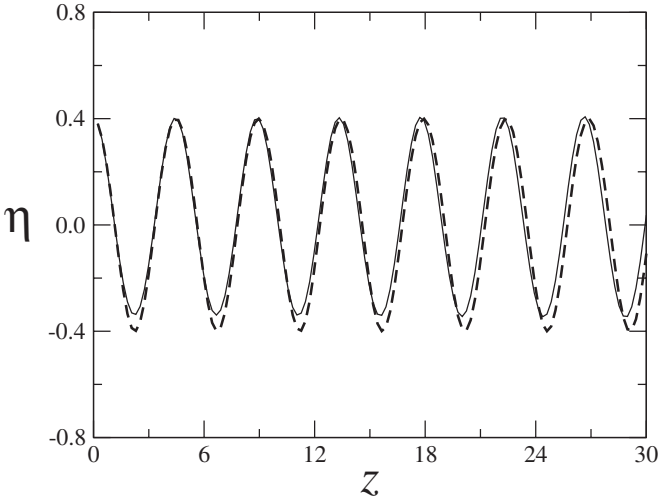

FIG. 2. Comparison of χ's obtained from the model and full simulations: χ_{model} is represented by the dotted line and the fully simulated $\chi_{\text{simulation}}$ by the solid line. All parameters and initial conditions as in the previous figure.

gone into halo formation. In this $\chi_0=0.4$ case for instance, wave breaking in crystalline distributions occurs at $z\sim 1500$, while in the presently analyzed thermal distribution particles already reached the bounding curve at $z\sim 200$ where the core still oscillates coherently.

As for halo structure of asymptotic states, results for the simulations are displayed in Fig. 3 where one sees the distribution of N_t beam macroparticles in phase space at the instant $z=5000$, where the system has already reached its stationary state. In the final relaxed state represented by the figure, one can clearly perceive a flat line extending up to the maximum radius $r=1(\approx r_c)$ with small thickness along the velocity axis, surrounded by a low density cloud of hot particles. This narrow flat line incorporates the idea of a cold core, and the hot cloud lies in the phase space in a similar manner as particles of the previous test particle computations, Fig. 1. The geometric layout of both figures is thus similar, but one must still run a final test where actual physical quantities are investigated. As mentioned earlier, we choose to examine emittance. The result is strikingly similar: while the test particle simulations revealed a emittance $\varepsilon_{\text{model}}=0.106$ for the particular $\chi_0=0.4$, our full simulations based on definition (13) for the relaxed emittance, attributes the value $\varepsilon_{\text{simulation}}=0.099$ to this quantity.

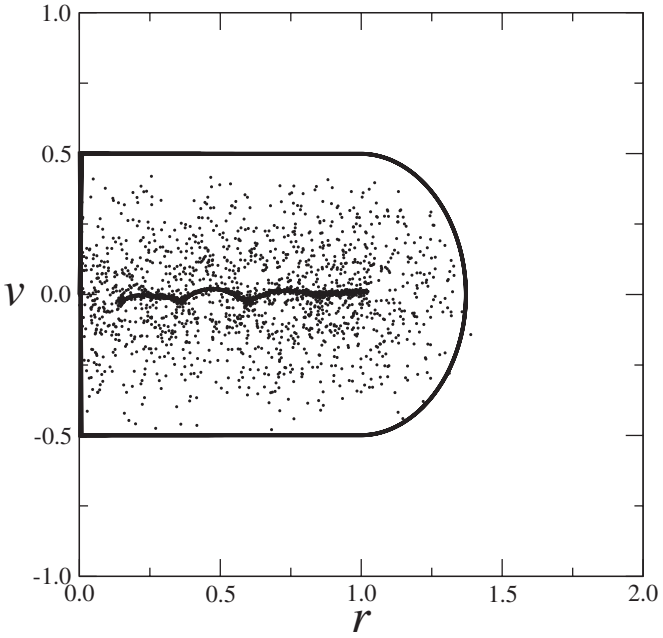

FIG. 3. Full simulations displaying a snapshot of the phase space occupied by $N_t=10\,000$ macroparticles at $z=5000$, for $\chi_0=0.4$. The thick line representing bounding energy is once again displayed.

TABLE I. Comparison of full simulations and analytical estimates for asymptotic states based on test particle dynamics and conserved quantities.

χ_0	$\varepsilon_{\text{analytical}}$	$\varepsilon_{\text{simulation}}$
0.2	0.053	0.051
0.4	0.106	0.099
0.6	0.152	0.140
0.8	0.211	0.175

Comparison between simulations and the model is further extended in Table I where we list a series of results for various values of the initial amplitude χ_0, always taking $\chi'(z=0)=0$ in the test particle simulations. We note that for all considered values of the inhomogeneity parameter χ_0 agreement between simulations and the low dimensional model remains tight.

IV. FINAL REMARKS

Combining techniques of Lagrangian fluids, average Lagrangians, test particle methods, and the expression for the conserved energy, we obtained an accurate description of halo formation in inhomogeneous beams. Particles are scattered off density fluctuations of the inhomogeneous core and form a low density population moving under the action of this core. Representing the low density population as test particles, and aided by the fact that energy is conserved, we then determined the final relaxed emittance of the system. The model was then compared with full self-consistent simulations and we found the results in nice agreement.

Our theory applies to space charge dominated beams where there is a small velocity spread with magnitude much smaller than the average fluid velocity. This amounts to the validity condition $0<\varepsilon(z=0)\ll v_{\text{directed}}$ in our dimensionless set of physical quantities where $r_b\sim 1$. v_{directed} can be estimated as we insert $n=n(r,\chi(z))$ from Eq. (6) into Eq. (5), with $\chi=\chi(z)$ provided by the average Lagrangian method. In our initial conditions we thus use slightly thermal beams where velocity dispersion is not larger than one-tenth of the maximum average velocity. Under these conditions particles detach early from the core while our ansatz is still accurate. The noteworthy point here is that the ansatz still provides a good quantitative agreement with simulations even in cases of crystalline beams, where particles begin to be ejected from the core only when wave breaking and the associated phase mismatches take place. In this situation where beam oscillations cannot be faithfully described in terms of our mono-

chromatic ansatz, the dominant frequency and amplitude predicted by the ansatz apparently suffices to provide a good picture of the test particle overall dynamics.

ACKNOWLEDGMENTS

This work is supported by CNPq and FAPERGS, Brazil, and by the (U.S.) Air Force Office of Scientific Research (AFOSR) under the Grant No. FA9550-06-1-0345. Part of the numerical work was carried out at the CESUP-UFRGS Supercomputing Center. Helpful comments by Chiping Chen are also acknowledged.

We dedicate this paper to the memory of our dear friend and colleague, Ruth de Souza Schneider.

[1] A. Cuchetti, M. Reiser, and T. Wangler, in *Proceedings of the Invited Papers, 14th Particle Accelerator Conference*, San Francisco, CA, 1991, edited by L. Lizama and J. Chew (IEEE, New York, 1991), Vol. 1, p. 251.
[2] R. L. Gluckstern, Phys. Rev. Lett. **73**, 1247 (1994).
[3] R. Pakter, G. Corso, T. S. Caetano, D. Dillenburg, and F. B. Rizzato, Phys. Plasmas **1**, 4099 (1994).
[4] R. Pakter, S. R. Lopes, and R. L. Viana, Physica D **110**, 277 (1997).
[5] S. M. Lund, D. P. Grote, and R. C. Davidson, Nucl. Instrum. Methods Phys. Res. A **544**, 472 (2005); Y. Fink, C. Chen, and W. P. Marable, Phys. Rev. E **55**, 7557 (1997).
[6] F. B. Rizzato, R. Pakter, and Y. Levin, Phys. Plasmas **14**, 110701 (2007).
[7] J. M. Dawson, Phys. Rev. **113**, 383 (1959).
[8] S. G. Anderson and J. B. Rosenzweig, Phys. Rev. ST Accel. Beams **3**, 094201 (2000).
[9] H. Okamoto and M. Ikegami, Phys. Rev. E **55**, 4694 (1997).
[10] M. Reiser, *Theory and Design of Charged Particle Beams* (Wiley-Interscience, New York, 1994); R. C. Davidson and H. Qin, *Physics of Intense Charged Particle Beams in High Energy Accelerators* (World Scientific, Singapore, 2001).
[11] R. Pakter and F. B. Rizzato, Phys. Rev. Lett. **87**, 044801 (2001).
[12] P. J. Morrison, Rev. Mod. Phys. **70**, 467 (1998).
[13] G. B. Witham, *Linear and Nonlinear Waves* (Wiley, New York, 1974).
[14] R. P. Nunes, R. Pakter, and F. B. Rizzato, J. Appl. Phys. **104**, 013302 (2008); Phys. Plasmas **14**, 023104 (2007).